2017

Accommodation of the human lens capsule using a finite element model based on nonlinear regionally anisotropic biomembranes

G. David
University of the Philippines

Ryan M. Pedrigi
University of Nebraska-Lincoln, rpedrigi@unl.edu

J. D. Humphrey
Yale University

Published in *Computer Methods in Biomechanics and Biomedical Engineering* 20:3 (2017), pp 302–307
doi 10.1080/10255842.2016.1228907

Submitted 18 August 2014; accepted 22 August 2016

Accommodation of the human lens capsule using a finite element model based on nonlinear regionally anisotropic biomembranes

G. David,[1] R. M. Pedrigi,[2] and J. D. Humphrey[3]

1 Institute of Mathematics, University of the Philippines, Quezon City, Philippines
2 Department of Bioengineering, Imperial College London, London, UK
3 Department of Biomedical Engineering, Yale University, New Haven, CT, USA

Corresponding author — G. David, *email* gdavid@science.upd.edu.ph

Abstract
Accommodation of the eyes, the mechanism that allows humans to focus their vision on near objects, naturally diminishes with age via presbyopia. People who have undergone cataract surgery, using current surgical methods and artificial lens implants, are also left without the ability to accommodate. The process of accommodation is generally well known; however the specific mechanical details have not been adequately explained due to difficulties and consequences of performing *in vivo* studies. Most studies have modeled the mechanics of accommodation under assumptions of a linearly elastic, isotropic, homogenous lens and lens capsule. Recent experimental and numerical studies showed that the lens capsule exhibits nonlinear elasticity and regional anisotropy. In this paper we present a numerical model of human accommodation using a membrane theory based finite element approach, incorporating recent findings on capsular properties. This study seeks to provide a novel perspective of the mechanics of accommodation. Such findings may prove significant in seeking biomedical solutions to restoring loss of visual power.

Keywords: Finite element method, ophthalmology, biomembranes, lens capsule accommodation

1. Introduction

The lens is a transparent, ellipsoidal-shaped, gel-like structure of the eye whose function is to focus light onto the retina at the back of the eye, similar to a lens in a telescope. The human lens changes shape by movement of the ciliary muscles, a process called accommodation, in order for us to adjust our vision to see near objects. The lens is composed mostly of protein and water, and is encased in the lens capsule, a thin membrane made up of collagen.

It has been more than a century and a half since von Helmholtz first proposed his theory of accommodation based on *in vivo* data. Ciliary muscles surrounding the lens and structural thin fibers called zonules that anchor the lens body to the ciliary muscles were thought to play a central role in the ability of the human eye to adjust for near or distant vision. Helmholtz' theory holds that when ciliary muscles relax, the zonules become subjected to tension, pulling the lens capsule along its equator and causing the lens body to flatten, thereby letting the eye see distant objects (Martin et al. 2005). When the ciliary muscles contract, the zonules are released from tension, causing the lens body to become more curved, allowing the eye to focus on nearby objects (Alpern 1969; Fisher 1969; Burd et al. 2002). An alternative theory of accommodation states that during accommodation, relaxing of the ciliary muscles cause the equatorial zonules to pull on the lens capsule, resulting in steepening of the central anterior region and flattening at the equator (Schachar 1992, 1999; Schachar et al. 1993; Schachar & Bax 2001; Chien et al. 2003; Schachar & Kamangar 2006).

An important factor in modeling accommodation accurately lies in the assumption of the mechanical properties of the associated tissues. Most numerical studies use data on the biomaterial properties of the lens capsule from Krag and Andreasen (1996, 2003a, 2003b) and Krag et al. (1997, 1997a, 1997b). Their work has been largely based on uniaxial tests on thin strips cut out from the lens capsule and their data presented in terms of linear elasticity. More recent work from our group revealed, however, that the lens capsule exhibits a nonlinear, regionally anisotropic behavior (Heistand et al. 2005; Heistand et al. 2006; David & Humphrey 2007; David et al. 2007; Pedrigi, David et al. 2007; Pedrigi, Staff et al. 2007). These data and findings are used as key assumptions in the present model of human lens accommodation.

The conventional way to model accommodation is to regard the lens as an elastic material and apply traction near the equator. An alternative approach is to model the lens capsule as a fluid-filled hyperelastic biomembrane. As the subject ages, the lens becomes increasingly stiffer, and this leads to presbyopia and a loss of the ability to accommodate.

2. Methods

The formulation below follows Gruttman and Taylor (1992) and Kyriacou et al. (1996). Let **X** be the 3-D initial position of a material particle on the surface of the anterior lens capsule, and let **x** be its corresponding 3-D deformed position. For numerical convenience, local orthogonal coordinates $\{s_i\}$ are defined, such that $\mathbf{X} = \mathbf{X}(s_1, s_2)$ and $\mathbf{x} = \mathbf{x}(s_1, s_2)$, with orthonormal bases

$$\mathbf{G}_j = \frac{\partial \mathbf{X}}{\partial s_j} \tag{1}$$

The right Cauchy–Green tensor (Humphrey 1998, 2002) is then calculated by

$$\mathbf{C} = \frac{\partial \mathbf{x}}{\partial s_\alpha} \frac{\partial \mathbf{x}}{\partial s_\beta} \; \mathbf{G}_\alpha \otimes \mathbf{G}_\beta \tag{2}$$

The inflation of the membrane is modeled here using the virtual work principle:

$$\int_{\Omega_0} \delta w \mathrm{d}A = \int_{\Omega} p\mathbf{n} \cdot \delta\mathbf{x} \mathrm{d}a - \int_{\partial\Omega} \mathbf{T} \cdot \delta\mathbf{x} \mathrm{d}a \tag{3}$$

where δw is the incremental strain energy function per undeformed area in the underformed or initial surface Ω_0, p is the distending pressure (in MPa), **n** is an outward unit normal vector, $\delta\mathbf{x}$ is a virtual displacement, and **T** is the force per area applied on some subdomain $\partial\Omega$ of the deformed surface Ω. Results from inverse subdomain finite element analysis suggested a good fit with biaxial data on the lens capsule using the Fung model (Fung 1990, 1993; Humphrey 1998, 2002; Seshaiyer & Humphrey 2003; David et al. 2007; Pedrigi, David et al. 2007):

$$w = \frac{c^k (\exp (c_1^k E_{11}^2 + c_2^k E_{22}^2 + 2c_3^k E_{11} E_{22}) - 1)}{2} \tag{4}$$

where c^k, c^k_1, c^k_2, c^k_3 are nonnegative material parameters for $k = a, p$ corresponding to the anterior and posterior capsules, respectively, and E_{ij} are components of the Green strain tensor, $\mathbf{E} = (\mathbf{C} - \mathbf{I})/2$ (David & Nabong 2015). The 1 and 2 subscripts denote circumferential and meridional directions, respectively, i.e. the principal directions in the lens capsule.

The lens capsule was assumed to be axially symmetric, i.e. its cross section is circular. Experimental data from human anterior lens capsule interpreted via the Fung model were nonlinear and regionally anisotropic. Material parameters varied with age. Here, we used representative values: $c_3^a = c_3^p = 0.5$, and $c^a = 1.5$N/m. Based on experiments (David & Humphrey 2007; Pedrigi, David et al. 2007), values for circumferential and meridional parameters varied with arc length s measured from the pole, given in mm. For consistency of units, s is rendered dimensionless by dividing by 1 mm. For the anterior capsule, the circumferential parameter $c^a{}_1(s)$ increased with s, i.e. away from the anterior pole towards the equator, whereas the meridional value $c^a{}_2(s)$ decreased from the pole towards the equator, with matching values at the pole, i.e. $c^a{}_1(0) = c^a{}_2(0)$. The properties below were inferred from data on the anterior lens capsule:

$$\frac{dc_1^a}{ds} > 0, \quad \frac{d_2c_1^a}{ds_2} > 0, \quad \frac{dc_2^a}{ds} < 0, \quad \lim_{s\to\infty} c_2^a = 0 \tag{5}$$

Normal regression on the data may result in a good fit, but using high order polynomials is not recommended. A simple material parameter profile that approximated the anterior capsule behavior while satisfying the conditions in (5) was given by:

$$c_1^a(s) = s_0 + 4s^2 \tag{6}$$

where s_0 is the stiffness at the pole, with an experimental value of $s_0 = 20$. The average meridional values appeared to follow a downward parabola. However, fitting a quadratic function with the meridional values is problematic because this implies the stiffness would become zero at some arc length. The following meridional parameter profile was used:

$$c_2^a(s) = \frac{5s_0}{(5 + s^2)} \tag{7}$$

Data for the posterior capsule were not obtained experimentally. We assumed $c^p{}_1 = c^a{}_1$, $c^p{}_2 = c^a{}_2$ and $c^p{}_3 = c^a{}_3$. For the overall stiffness, we used $c^p = c^a/3$ based on measurements of the posterior capsule thickness, which is typically 1/3 the thickness of the anterior capsule (David & Humphrey 2007; Pedrigi, David et al. 2007).

The 3-D geometry of the lens was generated by taking two nearly-flat quarter circular sheets of radius 4.8mm joined at the equator and applying pressure between the sheets, the upper sheet forming the anterior capsule and the lower sheet forming the posterior capsule. In the absence of pressure, we can think of the unpressurized geometry as the state of the lens capsule if it was placed on a flat surface and the lens was extracted, shown in **Figure 1**. The lens in the model behaved as a fluid, represented

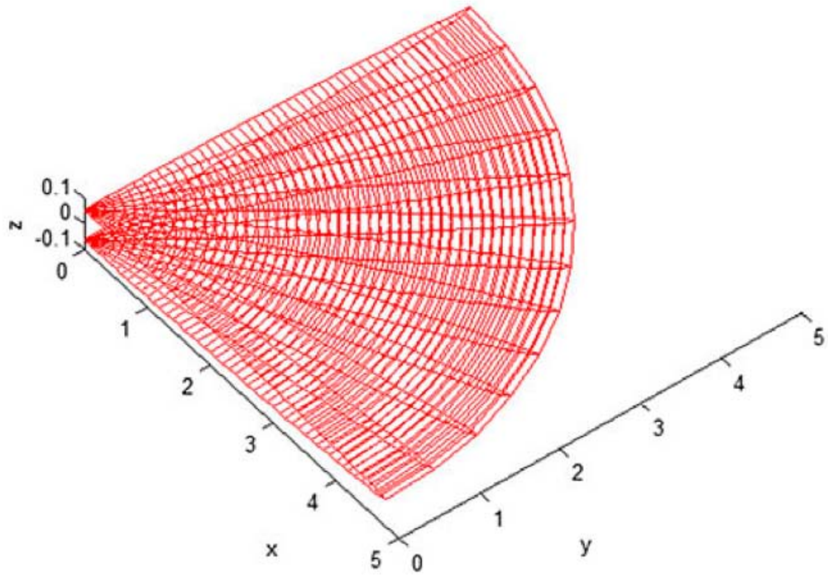

Figure 1. Nearly flat lens capsule quarter-model in the reference configuration at zero pressure, i.e. without the lens.

by internal pressure on the lens capsule. In the finite element model, the edges along the coordinate planes were given rolling boundary conditions, i.e. constrained to move along the plane.

3. Results and discussion

The pressure exerted by the lens on the lens capsule, based on experiments, is believed to be less than 5mmHg (David & Humphrey 2007; Pedrigi, David et al. 2007). External pressure on the lens capsule by intraocular fluid would reduce this pressure further. For the simulations, fluid pressure values of p = 4, 5 and 6mmHg, the latter for comparison, were used in (3) to model the accommodated (herein, the initial configuration) lens capsule. **Figure 2(a)** shows the lens capsule with internal pressure of p = 4 mmHg, denoting the fully accommodated lens. Note that regional anisotropy caused the lens capsule to inflate flatter than a sphere, which would be the expected geometry of an isotropic lens capsule.

The unaccommodated lens capsule in the model was the deformed configuration, obtained by simulating zonular tension via equatorial tractions. Shown in **Figure 2(b)** is the geometry obtained by first applying an internal pressure of p = 4mmHg and then applying traction of T = 0.06N/mm^2 along the equator. Note that the latter value of force per area, when applied on a

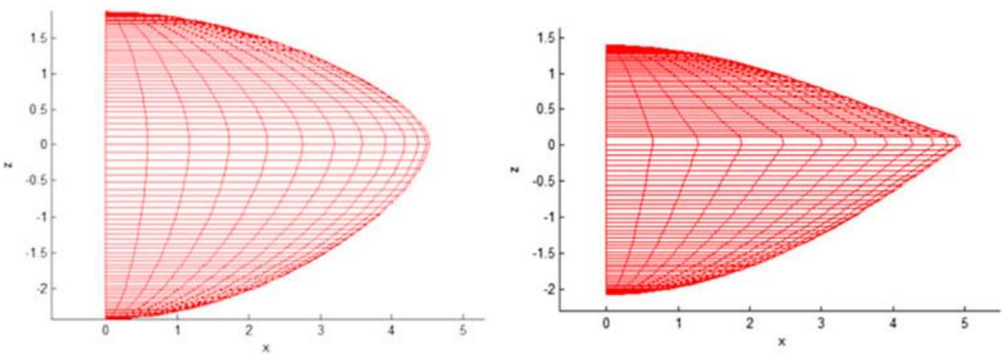

(a) Accommodated Lens (b) Unaccommodated Lens

Figure 2. Initial state (accommodated lens) simulated by applying internal pressure of p = 4 mmHg, and deformed state (unaccommodated lens) obtained by applying the same pressure and a traction of T = 0.06 N/mm^2 along the equator.

thin ring around the equator, is equivalent to a force of 0.04N, within the prescribed range (Fisher 1977; Burd et al. 2002; Hermans et al. 2006). The model did not consider the zonule forces acting on the anterior and posterior portions of the lens capsule (Burd, Judge & Flavell 1999; Burd et al. 2002).

For the accommodated lens with a pressure of 4mmHg, the anterior thickness of 1.87mm, posterior thickness of 2.42mm, and lens diameter of 9.05mmwere consistent with *in vivo* measurements and human lens models for middle aged humans (Dubbelman & Van der Heijde 2001; Dubbelman et al. 2001, 2003, 2005; Burd et al. 2002; Abolmaali et al. 2007; Schachar et al. 1996; Urs & Manns 2009). The radius of curvature was 6.98mm for the anterior and 5.62mm for the posterior lens capsule. These were consistent with measurements of an accommodated lens (Rosen et al. 2006; Hermans et al. 2007, 2009; Kasthurirangan et al. 2011; Lanchares et al. 2012). The geometry obtained using a pressure of 5–6mmHg had slightly greater thickness, but the dimensions were still within the range of measurements and human models (Augusteyn et al. 2011). The dimensions for the lens model with p = 4, 5, 6mmHg can be seen in **Figures 3, 4 and 5**(a).

Equatorial traction values up to T = 6N/mm_2, equivalent to an equatorial force of up to 4N, were applied on the lens capsule model for three pressure levels. The higher value was used as model for the unaccommodated lens. The resulting dimensions for p = 4 mmHg, with anterior and posterior thickness of 1.40–2.08 mm, diameter of 9.87 mm, and anterior and posterior radius of curvature of 9.32–6.33 mm, respectively, were also within the range of measurements and human lens accommodation models (Glasser & Campbell 1998; Burd et al. 2002; Augusteyn et al. 2011; Lanchares et al. 2012).

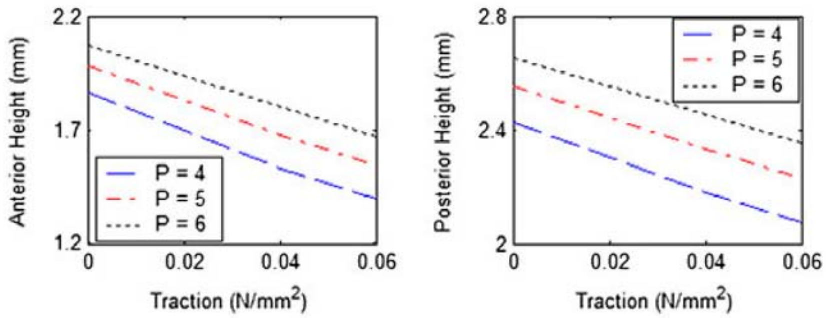

Figure 3. Anterior thickness (left, in mm) and posterior thickness (right, in mm) of lens capsule upon application of traction values up to T = 0.06 N/mm^2, for three assumed pressure levels: p = 4, 5, 6 mmHg.

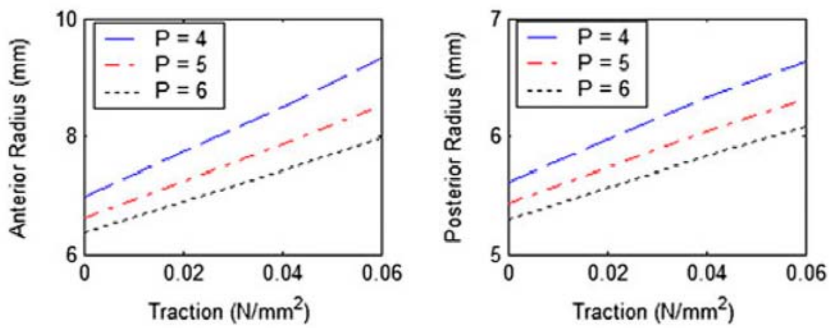

Figure 4. Anterior radius of curvature (left, in mm) and posterior radius of curvature (right, in mm) of lens capsule upon application of traction values up to 0.06 N/mm^2, for three assumed pressure levels: p = 4, 5, 6 mmHg.

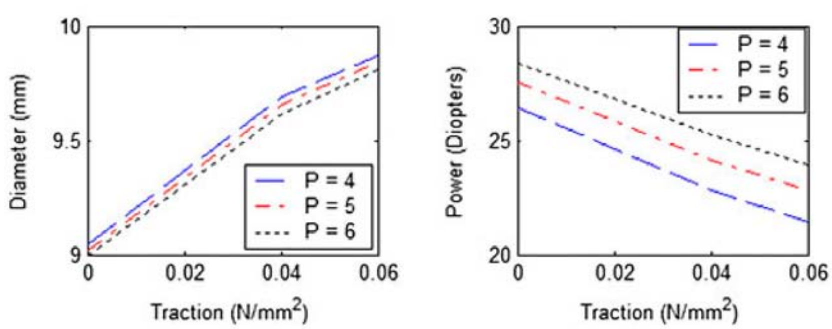

Figure 5. Diameter (left, in mm) and central optical power (in Diopters) of lens capsule upon application of traction values up to T = 0.06 N/mm^2, for three assumed pressure levels: p = 4, 5, 6 mmHg.

The central optical power was calculated using the following formula (Burd et al. 2002; Chien et al. 2003; Abolmaali et al. 2007):

$$P = \frac{n_l - n_a}{r_a} + \frac{n_l - n_a}{r_p} - \frac{h(n_l - n_a)^2}{r_a r_p n_l} \tag{8}$$

where the indices of refraction are given by $n_l = 1.42$, $n_a = 1.336$, h is the lens thickness (anterior plus posterior thickness) and r_a, r_p are the interior and posterior radius of curvature, respectively. The central optical power ranged from 26.43 to 28.36 Diopters for the accommodated lens capsule (T = 0 N/mm^2) and 21.41–23.92 Diopters for the unaccommodated lens capsule (T = 0.06N/mm^2) were also within range of studies on human lens accommodation (Glasser & Campbell 1998; Burd et al. 2002; Augusteyn et al. 2011). The optical power for p = 4, 5, 6 mmHg and equatorial traction up to 6 N/mm^2 are shown in Figure 5(b).

4. Conclusion

Accommodation of the human lens was numerically simulated via finite elements based on a membrane model for the lens capsule. In this model, the lens capsule acted as the primary mechanism involved in the accommodative process, while the lens pressurized the lens capsule similar to water in a balloon. The lens capsule material was endowed with regionally anisotropic material parameters based on the Fung material model, obtained experimentally. Inflating the initially flat, stress-free lens capsule with internal pressure of 4–5mmHg, equivalent to the pressure exerted by the lens on the lens capsule based on experimental data, caused the lens capsule to assume a geometry that approximated well dimensions of the lens in human eyes. Unaccommodating the lens model was performed by applying a traction along the equator equal to 0.06N/mm^2, equivalent to zonule force of 0.04N. The resulting thickness, diameter, radius of curvature and central optical power of the accommodated and unaccommodated lens capsules were in the range of *in vivo* measurements and other lens models.

Images of the human lens capsule indicate zonules located along the equator, as well as the anterior and posterior portions of the lens capsule. The present study assumed an equivalent net traction along the equator. This simplification has been used by other accommodation models. Future models may improve on this by considering the forces along the three zonule locations, which may help replicate Schachar's theory of accommodation. Nevertheless, the model presented herein is the first study on lens accommodation based on membrane theory that used regionally anisotropic material properties.

Disclosure — The authors report no potential conflict of interest.

Funding — This work was supported, in part, via a contract from Alcon Laboratories, Inc. (Fort Worth, Texas); and the University of the Philippines Creative Work and Research Program.

References

Abolmaali A, Schachar RA, Le T. 2007. Sensitivity study of human crystalline lens accommodation. Comput Methods Prog Biomed. 85:77–90.

Alpern M. 1969. Accommodation. In: Davson H, editor. The eye; muscular mechanisms. Vol. 3. New York (NY): Academic Press; p. 72–80.

Augusteyn RC, Mohamed A, Nankivil D, Veerendranath P, Arrieta E, Taneja M, Manns F, Ho A, Parel JM. 2011. Age-dependence of the optomechanical responses of *ex vivo* human lenses from India and the USA, and the force required to produce these in a lens stretcher: The similarity to *in vivo* disaccommodation. Vision Res. 51:1667–1678.

Burd HJ, Judge SJ, Cross JA. 2002. Numerical modelling of the accommodating lens. Vision Res. 42:2235–2251.

Burd HJ, Judge SJ, Flavell MJ. 1999. Mechanics of accommodation of the human eye. Vision Res. 39:1591–1595.

Chien CH, Huang T, Schachar RA. 2003. A mathematical expression for the human crystalline lens. Comput Thermodyn. 29:245–258.

David G, Humphrey JD. 2007. Finite element model of stresses in the anterior lens capsule of the eye. Comput Methods Biomech Biomed Eng. 10:237–243.

David G, Nabong JR. 2015. Rupture model of intracranial saccular aneurysms due to hypertension. J Mech Med Biol. 15:1550022-1–7.

David G, Pedrigi RM, Heistand MR, Humphrey JD. 2007. Regional multiaxial mechanical properties of the porcine anterior lens capsule. ASME J Biomech Eng. 129:97–104.

Dubbelman M, Van der Heijde GL. 2001. The shape of the aging human lens: curvature, equivalent refractive index and the lens paradox. Vision Res. 41:1867–1877.

Dubbelman M, Van der Heijde GL, Weeber HA. 2001. The thickness of the aging human lens obtained from corrected Scheimpflug images. Optometry Vision Sci. 78:411–416.

Dubbelman M, Van der Heijde GL, Weeber HA, Vrensen GF. 2003. Changes in the internal structure of the human crystalline lens with age and accommodation. Vision Res. 43:2363–2375.

Dubbelman M, Van der Heijde GL, Weeber HA. 2005. Change in shape of the aging human crystalline lens with accommodation. Vision Res. 45:117–132.

Fisher RF. 1969. Elastic constants of the human lens capsule. J Physiol. 201:1–19.

Fisher RF. 1977. The force of contraction of the human ciliary muscle during accommodation. J Physiol. 270:51–74.

Fung YC. 1990. Biomechanics: motion, flow, stress and growth. New York (NY): Springer-Verlag.

Fung YC. 1993. Biomechanics: mechanical properties of living tissue. New York (NY): Springer-Verlag.

Glasser A, Campbell MC. 1998. Presbyopia and the optical changes in the human crystalline lens with age. Vision Res. 38:209–229.

Gruttman F, Taylor RL. 1992. Theory and finite element formulation of rubber-like membrane shells using principal stretches. Int J Numer Methods Eng. 35:1111–1126.

Heistand MR, Pedrigi RM, Delange S, Dziezyc J, Humphrey JD. 2005.Multiaxial mechanical behavior of the porcine anterior lens capsule. Biomech Model Mechanobiol. 4:168–177.

Heistand MR, Pedrigi RM, Dziezyc J, Humphrey JD. 2006. Redistribution of strain in the porcine lens capsule due to a continuous circular capsulorhexis. J Biomech. 39:1537–1542.

Hermans EA, Dubbelman M, Van der Heijde GL, Heethaar RM. 2006. Estimating the external force acting on the human eye lens during accommodation by finite element modelling. Vision Res. 46:3642–3650.

Hermans EA, Dubbelman M, Van der Heijde GL, Heethaar HR. 2007. The shape of the human lens nucleus with accommodation. J Vision. 7:16.1–16.10.

Hermans EA, Pouwels PJW, Dubbelman M, Kuijer JPA, van der Heijde GL, Heethaar RM. 2009. Constant volume of the human lens and decrease in surface area of the capsular bag during accommodation: an MRI and Scheimpflug study. Invest Ophthalmol Vis Sci. 50:281–289.

Humphrey JD. 1998. Computer methods in membrane biomechanics. Comput Methods Biomech Biomed Eng. 1:171–210.

Humphrey JD. 2002. Cardiovascular solid mechanics: cells, tissues, and organs. New York (NY): Springer-Verlag.

Kasthurirangan S, Markwell EL, Atchison DA, Pope JM. 2011. MRI study of the changes in crystalline lens shape with accommodation and aging in humans. J Vision. 11:1–16.

Krag S, Andreasen TT. 1996. Biomechanical measurements of the porcine lens capsule. Exp Eye Res. 62:253–260.

Krag S, Andreasen TT. 2003a. Mechanical properties of the human lens capsule. Prog Retinal Eye Res. 22:749–767.

Krag S, Andreasen TT. 2003b. Mechanical properties of the human posterior lens capsule. Invest Ophthalmol Vis Sci. 44:691–696.

Krag S, Danielsen CC, Andreassen TT. 1997. Thermal and mechanical stability of the lens capsule. Curr Eye Res. 17: 470–477.

Krag S, Olsen T, Andreassen TT. 1997a. Biomechanical characteristics of the human anterior lens capsule in relation to age. Invest Ophthalmol Vis Sci. 38:357–363.

Krag S, Olsen T, Andreassen TT. 1997b. Viscoelastic properties of the human lens capsule. Invest Ophthalmol Vis Sci. 38:456–459.

Kyriacou SK, Schwab C, Humphrey JD. 1996. Finite element analysis of nonlinear orthotropic hyperelastic membranes. Comput Mech. 18:269–278.

Lanchares E, Navarro R, Calvo B. 2012. Hyperelastic modelling of the crystalline lens: Accommodation and presbyopia. J Optometry. 5:110–120.

Martin H, Guthoff R, Terwee T, SchmitzKP. 2005. Comparison of the accommodation theories of Coleman and of Helmholtz by finite element simulations. Vision Res. 45:2910–2915.

Pedrigi RM, David G, Ziezyc J, Humphrey JD. 2007. Regional mechanical properties and stress analysis of the human anterior lens capsule. Vision Res. 47:1781–1789.

Pedrigi RM, Staff E, David G, Glenn S, Humphrey JD. 2007. Altered multiaxial mechanical properties of the porcine anterior lens capsule cultured in high glucose media. J Biomech Eng. 129:121–125.

Rosen AM, Denham DB, Fernandez V, Borja D, Ho A, Manns F, Parel JM, Augusteyn RC. 2006. *In vitro* dimensions and curvatures of human lenses. Vision Res. 46:1002–1009.

Schachar RA. 1992. Cause and treatment of presbyopia with a method for increasing the amplitude of accommodation. Ann Ophthalmol. 24:445–449.

Schachar RA. 1999. Is Helmholtz's theory of accommodation correct? Ann Ophthalmol. 31:10–17.

Schachar RA, Bax AJ. 2001. Mechanism of human accommodation as analyzed by nonlinear finite element analysis. Compr Ther. 27:122–132.

Schachar RA, Huang T, Huang X. 1993. Mathematic proof of Schachar's hypothesis of accommodation. Ann Ophthalmol. 25:5–9.

Schachar RA, Kamangar F. 2006. Computer image analysis of ultrasound biomicroscopy of primate accommodation. Eye. 20:226–233.

Schachar RA, Tello C, Cudmore DP, Liebmann JM, Black TD, Ritch R. 1996. *In vivo* increase of the human lens equatorial diameter during accommodation. Am J Physiol. 271: 670–676.

Seshaiyer P, Humphrey JD. 2003. A subdomain inverse finite element characterization of hyperelastic membranes including soft tissues. J Biomech. 125:363–371.

Urs R, Manns F. 2009. Shape of the isolated *ex-vivo* human crystalline lens. Vision Res. 49:74–83.